

# Wavelength References for 1300-nm Wavelength-Division Multiplexing

T. Dennis, *Member, OSA*, E. A. Curtis, C. W. Oates, *Member, OSA*,  
L. Hollberg, *Associate Member, IEEE, Member, OSA*, and S. L. Gilbert, *Member, OSA*

**Abstract**—We have conducted a study of potential wavelength calibration references for use as both moderate-accuracy transfer standards and high-accuracy National Institute of Standards and Technology (NIST) internal references in the 1280–1320-nm wavelength-division-multiplexing region. We found that most atomic and molecular absorption lines in this region are not ideal for use as wavelength references owing to factors such as weak absorption, complex spectra, or special requirements (for example, frequency-doubling or excitation with an additional light or discharge source). We have demonstrated one of the simpler schemes consisting of a tunable diode laser stabilized to a Doppler-broadened methane absorption line. By conducting a beat-note comparison of this reference to a calcium-based optical frequency standard, we measured the methane line center with an expanded uncertainty ( $2\sigma$ ) of  $\pm 2.3$  MHz. This methane-stabilized laser now serves as a NIST internal reference.

**Index Terms**—Absorbing media, optical fiber communication, optical materials, optical propagation in absorbing media, optical spectroscopy, semiconductor lasers, standards, wavelength-division multiplexing.

## I. INTRODUCTION

WAVELENGTH-division multiplexing (WDM) is rapidly expanding the capacity of optical fiber communications systems. Current systems operate in the 1540–1560-nm region, but WDM will likely expand into other wavelength regions as well, possibly covering the entire range from about 1280 to 1630 nm. Wavelength calibration references are needed to calibrate instrumentation and reliably separate densely spaced channels in these new regions. Following the development of wavelength calibration references in the 1510–1560-nm region [1]–[3] and the WDM L-band (approximately 1565–1625 nm) [4], we have begun to investigate potential wavelength references in the 1300-nm region.

Our goals are to produce high-accuracy references for National Institute of Standards and Technology (NIST) internal calibration and moderate-accuracy transfer standards (such as NIST Standard Reference Materials) to help industry calibrate instrumentation. A wavelength reference for calibration in a standards laboratory should have a frequency uncertainty of less than 10 MHz, whereas a transfer standard can have an uncertainty of a few hundred megahertz. Atomic and molecular ab-

sorption lines provide wavelength references that are very stable under changing environmental conditions and have well understood physical behavior. A variety of molecules have distinctive absorption features in the 1300-nm region due to their quantized vibrational and rotational motion. These transitions are combination or overtone bands that can be probed directly, but they typically have low absorption strengths. Atomic transitions in this region occur between excited states and, thus, require initial excitation by a laser or electric discharge. Other atomic or molecular references can be realized by frequency doubling 1300-nm light to probe atomic transitions in the 650-nm region. Depending on the physical conditions of the reference and the measurement technique, a wide range of absorption linewidths can be realized. For example, a molecular or atomic gas at a pressure of 1 kPa (8 torr) typically has transition linewidths of less than 1 GHz that are dominated by Doppler broadening. On the other hand, a gas at a pressure of 100 kPa ( $\sim 1$  atmosphere) can have pressure-broadened linewidths of more than 10 GHz. Reductions in the linewidth below the Doppler limit, to widths of 10 MHz or less, can be realized with saturated absorption spectroscopy. For weak molecular transitions, this technique often requires a resonant cavity to increase the laser power.

We have conducted a survey of potential wavelength calibration references for use as moderate-accuracy transfer standards and high-accuracy NIST internal references in the 1280–1320-nm WDM region. We then produced a high-accuracy reference using one of the simpler schemes consisting of a tunable diode laser stabilized to a Doppler-broadened methane absorption line. In Section II, we present the results of our survey of potential references. In Section III, we describe the methane-based wavelength reference that we constructed and compared to a calcium-based optical frequency standard.

## II. REFERENCES IN THE 1300-nm REGION

Table I summarizes the atomic and molecular species we have considered as wavelength references for the 1280–1320-nm region. This range includes and is centered upon the gain spectrum of currently available praseodymium-doped fiber amplifiers. Some materials have been listed with specific transitions and wavelengths, while others are listed with band designations and wavelength ranges owing to the complexity of the molecular spectra. In some cases, weaker transitions and/or ones of lower accuracy have been omitted in spectrally dense regions. The uncertainty of the specified transitions or bands are given as fractions, where  $1 \times 10^{-6}$  at 1300 nm is equivalent to 230 MHz, 1.3 pm, and  $8 \times 10^{-3} \text{ cm}^{-1}$ . The column of special notes lists

Manuscript received October 23, 2001; revised February 26, 2002.

T. Dennis, C. W. Oates, L. Hollberg, and S. L. Gilbert are with the National Institute of Standards and Technology, Boulder, CO 80305 USA.

E. A. Curtis is with the National Institute of Standards and Technology, Boulder, CO 80305 USA and also with the Physics Department, University of Colorado at Boulder, Boulder, CO 80309 USA.

Publisher Item Identifier S 0733-8724(02)05119-8.

TABLE I  
SUMMARY OF MATERIALS FOR WAVELENGTH REFERENCES AT 1300 nm

Material	Transitions or bands	Wavelength (nm)	Fractional Uncertainty $\times 10^6$	Special Notes	Ref.
Rubidium	$5P_{1/2} \rightarrow 6S_{1/2}$	1323.87	0.2	Between excited states	5, 6, 7
Neon	$2p_4 \rightarrow 2s_5$	1291.56		Discharge	8, 9
Argon	$2p_8 \rightarrow 3d_1''$	1280.63		Discharge	8, 9, 10
	$2p_4 \rightarrow 2s_3$	1293.68			
	$2p_{10} \rightarrow 3d_5$	1296.03			
	$2p_3 \rightarrow 2s_2$	1301.19			
Krypton	$1s_3 \rightarrow 2p_7$	1286.54		Discharge	8, 9
	$2p_{10} \rightarrow 3d_1''$	1298.89			
	$2p_8 \rightarrow 2s_4$	1318.10			
Iodine	$X \rightarrow B$	11 calibration lines: 642.05 to 656.45	0.002	Heating, freq. doubling required	11, 12
Carbon Dioxide	R and P lines of $401_{II} \leftarrow 000$ ,	1286.52 to 1300.78,	3	Weak lines	13
	R and P lines of $401_{III} \leftarrow 000$	1311.83 to 1319.97			
Water	(002), (101), (200), (021), (120) $\leftarrow$ (000)	Hundreds of lines: 1280 to 1320	0.01	Heating required, complex spectrum	14, 15, 16
Acetylene	(1012 <sup>0</sup> ), (1012 <sup>2</sup> 0) <sub>c</sub>	69 lines: 1290.13 to 1306.17	0.4	Weak lines	16, 17, 18
Ammonia	(1110)	4 lines: 1293.34 to 1294.21	0.3	Likely Complex Spectrum	16
Nitrate rad. NO <sub>3</sub>	${}^2A'_1 - {}^2A'_2$ of ${}^2E'' - \bar{X}^2A'_2$	Hundreds of lines: 1315 to 1320	0.1	Complex Spectrum	19
Hydrogen Fluoride	R(0), P(1)-P(4)	5 lines: 1283.87 to 1321.24	0.2	Corrosive	20, 21
Hydrogen Sulfide	(102),(201), (300),(003)	300 lines: 1280 to 1320	$\geq 2.6$	Toxic	22
Methane	R(6) to R(9) of $\nu_2 + 2\nu_3$	Numerous lines: 1312 to 1320	4		15, 23

some of the principle experimental difficulties that would be encountered when working with a material.

The rubidium atom has been used extensively in high-resolution spectroscopy. The D2 transition at 780 nm forms a convenient 1560-nm reference through frequency-doubling [5], and serves as a NIST high-accuracy reference for this WDM region [1], [2]. A possibility for a 1300-nm reference is the  $5P_{1/2} \rightarrow 6S_{1/2}$  transition occurring at 1323.87 nm between excited states [6]. This transition is slightly outside the desired wavelength region, and stabilized optical pumping of the  $5P_{1/2}$  state is required. However, in one experiment a distributed-feedback diode laser has been locked to this transition [7].

The noble gases neon, argon, krypton, and xenon have been studied extensively as wavelength references in the 1300- and 1550-nm regions [8]–[10]. The materials have benign physical properties and offer a wide choice of absorption lines, as shown in the table (all the xenon transitions lie outside our region of interest). Unfortunately, all the noble gas transitions occur between excited states, typically requiring a high voltage discharge of the gas. This rather chaotic excitation process may be acceptable for moderate-accuracy references, but a detailed characterization of the discharge parameters and wavelength shifts would likely be required for a high-accuracy system.

Despite its simple chemical structure, the iodine molecule has an extremely complicated spectrum with more than 20 000 visible absorption lines in the X  $\rightarrow$  B band. A variety of gas lasers in the visible spectrum have been stabilized to these transitions, most notably the helium–neon laser at 633 nm. Frequency doubling would allow a 1300-nm laser to be referenced to one of these lines. A select number of appropriate lines have been measured to very high accuracy, with hyperfine components identified [11]. Doppler-limited locking to iodine has been performed using periodically poled lithium niobate and an Nd:YAG laser at 1319 nm [12]. In addition to efficient frequency doubling, this scheme requires moderate heating to increase the vapor pressure of iodine and populate higher vibrational levels of the ground state.

The common atmospheric molecules of carbon dioxide and water have been studied extensively with a combination of Fourier transform spectroscopy and theoretical calculations [13], [14]. Most of the absorption lines in the 1300-nm region are combinations or overtones of fundamental transitions at longer wavelengths, causing the line strengths to be weak. As a result, required absorption paths are long, often tens to hundreds of meters, and resonant cavities are a necessity for saturated absorption spectroscopy. Compared to water, the spectrum of carbon dioxide is simple and the lines are easily

identified, although they are about a factor of 100 weaker in strength [13]. Absorption lines of water have been used for spectroscopic calibration [15], [16]; moderate heating to increase vapor pressure may be necessary.

We also considered the molecules acetylene, ammonia, and the nitrate radical  $\text{NO}_3$ . Acetylene, which forms a convenient wavelength reference and is used as a NIST Standard Reference Material (SRM) between 1513 and 1541 nm [2], [3], has weak combination transitions near 1300 nm that require absorption paths of 30 m or more [17]. Even in the 1500-nm region, where the transitions are stronger, acetylene requires resonant cavities for saturated absorption spectroscopy [18]. There appear to be few studies of ammonia at 1300 nm; the long absorption path that was reported in one investigation is indicative of weak spectral features [16]. Also, based on spectra collected between 1450 and 1550 nm, the spectrum at 1300 nm is likely to be far more complicated than indicated by the four lines that have been reported. The nitrate radical  $\text{NO}_3$  has been the subject of numerous studies of chemical structure primarily involving spectroscopy at visible wavelengths. One study does report on hundreds of spectral features at wavelengths above 1315 nm; interestingly, water spectra were used for wavelength calibration in that study [19].

Hydrogen fluoride is a rare example of a molecule that offers strong absorption lines in the 1300-nm region [20]. While the lines are several orders of magnitude stronger than those of water, there are only five located between 1280 and 1320 nm. The primary disadvantage of this material is its high reactivity, which causes handling difficulties. Most absorption cells for hydrogen fluoride have been constructed of metal or plastic with sapphire or polyethylene windows. Despite this technical difficulty, diode laser stabilization to the R-branch lines has been demonstrated [21].

The hydrogen sulfide molecule offers several hundred lines in the 1300-nm region, but most of the detailed spectroscopy has been performed at wavelengths beyond 1600 nm. Therefore, information at shorter wavelengths on this toxic molecule is limited. In one relevant study, a Fourier transform spectrometer has been used to identify the bands near 1300 nm, determine the band center wavelengths, and count the number of lines within the bands [22]. The long absorption paths used by the study (28 and 433 m) indicate that the lines are weak. Because individual line positions have not yet been reported, detailed spectroscopy would be necessary to form a wavelength reference from this material.

Methane has been studied extensively with infrared spectroscopy to monitor gaseous concentrations in industrial environments, where it poses a high explosion danger, and in the atmosphere where it could be important to global warming. Detection of trace gases requires moderate wavelength accuracy to identify a species, placing higher emphasis on the accurate measurement of absorption depth, which is used to determine gas concentration. For this reason, the wavelength accuracy of previous studies would need to be improved to form a high-accuracy reference. The R branch lines of the  $\nu_2 + 2\nu_3$  band of methane, extending from 1314 to 1329 nm, are well suited for telecommunications wavelength references [15]. Unfortunately, the region below 1314 nm lacks any significant

absorption features. Nevertheless, methane is a good reference material because the R branch lines are reasonably strong, requiring absorption paths of less than 1 m, and can be probed at room temperature and low pressures. The relative ease with which the methane spectroscopy can be performed allows for the construction of an experimental apparatus that is compact, portable, and robust. Furthermore, methane is easy to handle in the laboratory, is readily available commercially with high purity, and can be safely contained in glass cells. Based on a report of Doppler-free spectroscopy in the 1600-nm region [23], saturation of the lines at 1300 nm should be possible using a resonant cavity. In comparison to the clean spectra of acetylene and hydrogen cyanide used for NIST SRMs in the 1500-nm region, the spectrum of methane is somewhat complicated. This is not a serious concern for a high-accuracy reference because the detailed structure can be resolved at lower pressures.

Based on the factors discussed in this section, we decided to produce a high-accuracy wavelength reference using a Doppler-broadened methane absorption line. This provides a relatively simple reference that could be measured relative to a highly accurate calcium frequency standard.

### III. METHANE HIGH-ACCURACY REFERENCE

Our development of a high-accuracy reference based on a methane absorption line near 1314 nm involved two parts: 1) stabilization of a diode laser to the methane line and 2) the accurate measurement of the frequency of the stabilized laser. The latter was necessary because we require a reference with a fractional uncertainty of less than  $1 \times 10^{-7}$ , but the methane lines had only been reported previously with an uncertainty of  $4 \times 10^{-6}$ . The frequency measurement was accomplished by conducting a beat-note measurement of the methane-stabilized laser with a laser referenced to a calcium-based optical frequency standard developed at NIST.

#### A. Experimental Setup

Fig. 1 shows the components of the methane-stabilized wavelength reference we constructed. We used a commercially available extended-cavity diode laser (ECDL) system having a 100-nm tuning range centered at 1304 nm. The laser linewidth was measured to be less than 5 MHz in a 50-ms interval with a Fabry-Pérot spectrum analyzer. The free-space beam of the tunable laser was passed through a bulk isolator before it was coupled into the FC/APC connector of a single-mode optical fiber. The laser power was then passed through a fiber isolator and divided by a fiber splitter, routing approximately 15% of the power to the methane stabilization components and 85% to a beat-note system for the measurement of the laser frequency. The portion of the laser beam used for methane stabilization was collimated into a free-space beam and divided by a wedged beam splitter. One part was directed to a photodiode to monitor intensity while the other passed through the methane gas cell to the signal photodiode. Common-mode intensity variations, such as those due to fluctuations in laser power and to etalon fringes associated with the diode laser chip and the free-space isolator, were removed from the methane spectra by subtracting

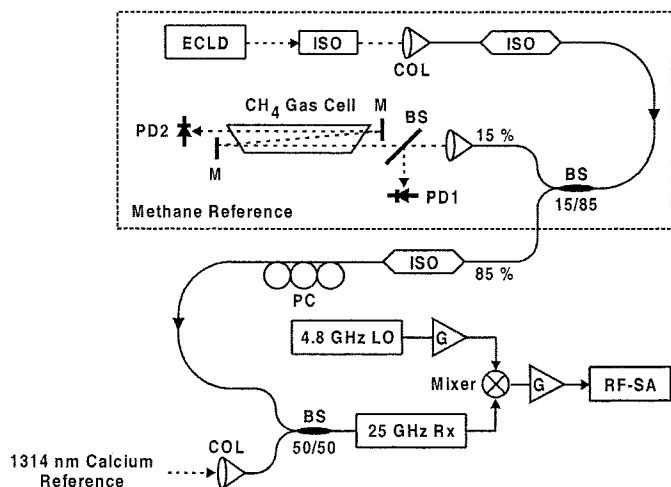


Fig. 1. The 1314-nm methane-stabilized laser and beat-note measurement system. ECDL: extended cavity laser diode. ISO: isolator. COL: fiber collimator. BS: beamsplitter. PD1, PD2: photodiodes. PC: polarization controller. RX: photoreceiver. LO: local oscillator. RF-SA: radio-frequency spectrum analyzer. G: electrical gain. The dashed signal paths represent free-space optical beams and the solid paths indicate fiber or electrical connections.

the photodiode signals. This improved the signal-to-noise ratio (SNR) and reduced the sensitivity of the stabilization lock-point to shifts of the fringes caused by temperature fluctuations and thermal expansion. Also, the windows of the gas cell were wedged to avoid production of interference fringes. To increase the absorption, the free-space beam traversed the cell three times for a total path of 60 cm. The entire optical and electrical system that formed the methane reference was designed to fit on a small pushcart to facilitate the beat-note measurements with the calcium frequency standard.

Fig. 2 shows a transmission spectrum of methane recorded by an optical spectrum analyzer, with the major R-branch lines identified. Even at a resolution of 15 pm and a relatively high gas pressure of 52.0 kPa (390 torr), it is clear that the spectrum of methane is complicated, with most lines possessing substructure. Despite the singlet appearance of R(3) in Fig. 2, a detailed laser scan at 0.3-pm resolution and 6.7 kPa (50 torr) revealed that it is actually a triplet line with features separated by about 12 pm. By contrast, the R(1) line was found to be a singlet under the same experimental conditions.

We dithered the center frequency of the laser by  $\pm 15$  MHz using a 1.6-kHz external modulation signal applied to the laser's piezoelectric tuning element. When the laser wavelength was slowly tuned across an absorption line and the photodiode signals were monitored with phase-sensitive detection at this modulation frequency, the derivative of the line shape was mapped. Fig. 3 shows derivative spectroscopy of the central feature of the R(8) cluster of lines at a pressure of 1.35 kPa (10.1 torr). Here, the laser was tuned in  $\sim 0.3$ -pm wavelength steps while the phase-sensitive detection signal was recorded in a 60-Hz bandwidth. With the wavelength stepping turned off and the modulated laser tuned near the center of an absorption line, the bipolar derivative signal represented the offset (error) of the laser from the zero crossing at line center. This normalized error signal was conditioned with integral and proportional feedback circuits and

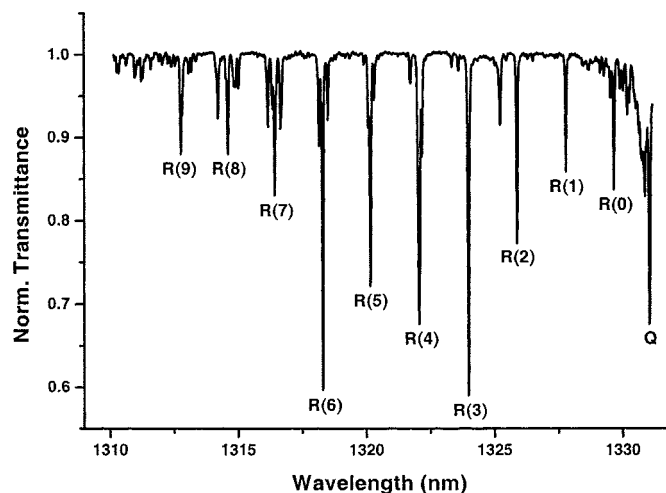


Fig. 2. Spectrum of the R-branch of methane at 52.0 kPa (390 torr) collected at a resolution of 15 pm on a vacuum wavelength scale. The spectrum is complex; most lines shown have substructure when viewed at higher resolution and lower pressure.

applied to the laser in summation with the external frequency modulation. Increasing the gain of the feedback circuit forced the laser to minimize the error signal, locking the wavelength to the center of the absorption line.

We locked the diode laser to the zero crossing at 1314.588 nm (vacuum wavelength) in the R(8) cluster of lines shown in Fig. 3. At low to moderate pressure, this line is sufficiently distinct that the wings of the two neighboring features at longer wavelengths have negligible effect on the lock point. We also confirmed with computer modeling that the small feature at 10 pm toward longer wavelength causes a negligible shift of the lock point of about 300 kHz. The 1314.588-nm feature was also the cleanest line in reasonable proximity ( $\sim 0.3$  nm) to the calcium-based optical frequency standard, resulting in a beat-note frequency that could be measured in the microwave range.

To characterize the pressure shift of this methane line, we stabilized the laser at two gas pressures using interchangeable cells with low (1.35 kPa; 10.1 torr) and high (8.21 kPa; 61.6 torr) pressures. The absorption depth of the line at the low and high pressures was 2% and 8%, respectively. We also collected absorption spectra of the stabilization feature at the two pressures and fitted the results to a Voigt line shape to characterize the pressure broadening. The low-pressure linewidth was essentially equal to the 720-MHz Doppler-broadened value while the high-pressure line was broadened slightly to 780 MHz. By contrast, the lines of Fig. 2 at an even higher pressure of 52.0 kPa (390 torr) have widths of about 2.8 GHz.

### B. Frequency Measurement

To accurately measure the frequency of the methane-stabilized laser, we compared it to a frequency-doubled 1314-nm laser that was locked to an optical frequency standard based on laser-cooled calcium atoms. The calcium frequency standard has been described in detail elsewhere [24]. In summary, it consists of an ECDL locked to the narrow (400-Hz natural linewidth)  $^1S_0 (m = 0) \rightarrow ^3P_1 (m = 0)$  transition at 657

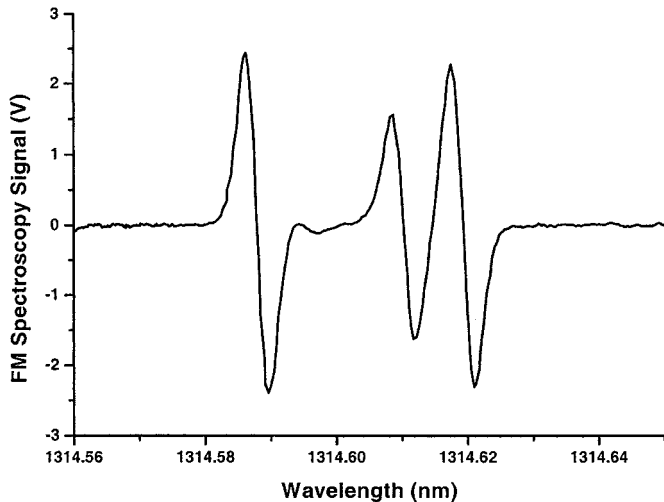


Fig. 3. Derivative spectroscopy signal of the central feature of the R(8) line plotted versus vacuum wavelength. The feature with a zero crossing at 1314.588 nm was used to create the methane-stabilized reference.

nm in neutral calcium. In order to achieve subkilohertz spectroscopic resolution and greatly reduced systematic shifts, this standard uses laser-cooled atoms from a magneto-optic trap operating at 423 nm. Recent measurements of the absolute frequency of a laser locked to this transition yielded an uncertainty of 26 Hz at 657 nm, corresponding to 13 Hz at 1314 nm [25]. This obviously far exceeds the requirements of a wavelength reference for WDM communications. The second harmonic of an ECDL at 1314 nm (different from the methane-stabilized laser and not shown in Fig. 1) was offset phase-locked to the calcium optical standard. By single-passing a periodically poled LiNbO<sub>3</sub> crystal with 5 mW of infrared light, more than 300 nW of second harmonic light at 657 nm was generated for use in the phase-lock beat signal. The remaining 1314-nm ECDL output (> 3 mW) was then available for generating a beat note with the methane-stabilized system.

The components of the beat-note measurement system used for the comparison are shown in the lower half of Fig. 1. The two sources were combined with a 3-dB optical fiber coupler, resulting in about 1 mW of optical power from each source. The fiber from the methane reference contained a fiber polarization controller to match the two polarization states. Combining the two sources on the photoreceiver allowed the 225-THz optical carriers to beat, producing an electrical signal at a difference frequency of about 57 GHz. The photoreceiver had a 3-dB bandwidth of 25 GHz, with a measured response at 50 GHz attenuated an additional 9 dB. We sent the output of the photoreceiver to a harmonic mixer, which mixed the input with harmonics it generated from the narrow-band signal of a synthesized local oscillator (LO). The mixing process shifted the center frequency of the beat note to less than 200 MHz, where it could be readily measured on a radio-frequency spectrum analyzer.

Fig. 4 shows a typical mixed-down beat-note signal recorded by the RF spectrum analyzer while the methane-stabilized reference was locked to the high-pressure methane cell. The signal was collected with a sweep time of 5 s at a resolution bandwidth of 1 MHz. The ~30-MHz width of the spectrum was

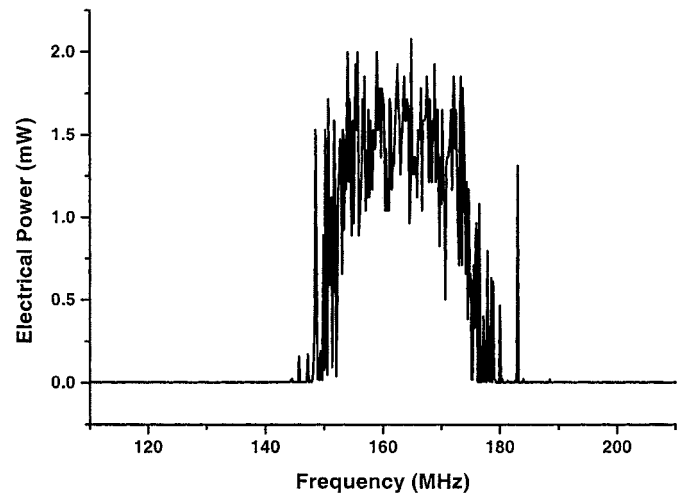


Fig. 4. Typical heterodyne beat spectrum between the 1314-nm laser locked to the methane line and the calcium-based frequency reference. The methane cell pressure was 8.21 kPa (61.6 torr). The mixed-down beat note was viewed on a RF spectrum analyzer with a 5-s sweep time and a 1-MHz resolution bandwidth. A center frequency of 163.0 MHz was obtained from this spectrum with a Gaussian curve fit.

caused by the large frequency dither needed to lock the laser diode to the Doppler-broadened methane line. In addition to the dither occurring at a rate of 1.6 kHz, the beat note also had a slower frequency jitter of about 10 MHz occurring on a time scale of more than 5 s. We suspect that this was due to a combination of the noise in the laser driver and the limitations of the feedback locking circuit. Unfortunately, the broad spectral width of the signal in combination with the moderate SNR of ~19 dB (in a detection bandwidth of 200 MHz) made electronic counting of the center frequency unreliable. Instead, we obtained a center value of 163.0 MHz for the signal of Fig. 4 by applying a Gaussian curve fit.

The frequency of the local oscillator driving the harmonic mixer during the measurement had a value of  $f_{LO} = 4794.887$  MHz, as measured by an electronic counter. The order of the harmonic that was mixing with the beat note was determined by dividing the ~57-GHz separation of the lasers by  $f_{LO}$ . The order was also determined by observing the difference between two different local oscillator frequencies that gave the same center frequency for the mixed-down beat note. From these two observations, we conclude that the 12th harmonic of  $f_{LO}$  was mixing with the 57-GHz beat note produced by the photoreceiver. Because the center frequency of the mixed-down beat note increased as  $f_{LO}$  increased, the 12th harmonic of the local oscillator was situated above the beat frequency. Therefore, the center frequency of the beat note of Fig. 4 before mixing was  $f_b = 12 \times 4794.887 \text{ MHz} - 163.0 \text{ MHz} = 57375.6 \text{ MHz}$ .

The absolute measurement of the frequency of the methane-stabilized laser was accomplished by accounting for two frequency offsets of the 1314-nm calcium-referenced laser with respect to the calcium line center. The probe laser at 657 nm was locked to the calcium line with an 80.0-MHz offset while 55.0 MHz separated the doubled 1314-nm light from the probe laser. Also, the methane absorption line at 1314.588 nm resides at a higher frequency than the calcium-based reference at 1314.919

TABLE II  
MEASURED FREQUENCIES AND CALCULATED WAVELENGTHS FOR THE METHANE REFERENCE,  
WITH EXPANDED UNCERTAINTIES ( $2\sigma$ )

Methane Pressure	Center Frequency	Center Wavelength (in vacuum)
$8.21 \pm 0.76$ kPa ( $61.6 \pm 5.8$ torr)	$228,050,483.1 \pm 2.3$ MHz	$1314.588129 \pm 0.000013$ nm
$1.35 \pm 0.12$ kPa ( $10.1 \pm 0.9$ torr)	$228,050,532.5 \pm 3.8$ MHz	$1314.587845 \pm 0.000022$ nm
Extrapolation to 0.00 kPa	$228,050,542.1 \pm 4.8$ MHz	$1314.587789 \pm 0.000028$ nm

nm. Considering all this, the absolute frequency of the methane wavelength reference is given by

$$f_{\text{methane}} = 1/2(f_{\text{Ca}} - 80.0 \text{ MHz} + 55.0 \text{ MHz}) + f_b$$

where  $f_{\text{Ca}} = 455\,986\,240.5$  MHz is the calcium transition frequency. The beat-note measurement and analysis were repeated with the laser stabilized to the low-pressure methane cell.

The stability characteristics of the methane-stabilized laser were tested in several ways. To demonstrate repeatability, beat-note measurements were performed again two days later, during a different part of the laboratory's daily temperature cycle (approximately a few degree Celsius). On each day, the beat note was measured up to ten times to obtain daily averages; we observed differences in the daily averages of about 1.1 MHz for both the high- and low-pressure cells. The temperature sensitivity was investigated in more detail by heating components of the system. Temperature changes of up to 5 °C did not cause observable shifts of the beat note frequency. If there was an effect due to temperature it was negligible relative to the random uncertainty. We also unlocked and relocked the diode laser a number of times to demonstrate short-term repeatability, and we varied parameters such as the amount of dither and feedback gain. In all cases, the wavelength reference remained consistent, with fluctuations that were within the uncertainty of the beat-note measurement.

Table II summarizes the absolute measurement results of center frequency for the methane reference at 1314.588 nm. By comparing the high- and low-pressure center frequencies, we conclude that a 6.87-kPa (51.5 torr) reduction in pressure resulted in a 49.4-MHz shift of the spectroscopic feature toward higher frequency. Assuming the pressure shift is linear, the slope is  $-7.2 \pm 1.1$  MHz/kPa ( $-0.96 \pm 0.14$  MHz/torr). The table also shows the position of the spectroscopic feature without the pressure shift, as determined by a linear extrapolation to zero pressure. The corresponding center wavelengths in vacuum were calculated using the defined value for the speed of light ( $c = 299\,792\,458$  m/s).

The uncertainties reported in Table II are the expanded uncertainties with a coverage factor of 2 (i.e., our values are  $2\sigma$ ), and were estimated from a variety of sources. A significant contribution to the frequency uncertainties for the high- and low-pressure cells originates from the standard deviation of the measurements. The center frequency of the high-pressure cell is the average of 30 measurements, with a standard deviation of 1.0 MHz. The low-pressure value is the result of 16 measurements with a standard deviation of 1.1 MHz. Both of the standard deviations (of the distributions) account for the daily repeatability, the temperature dependent variation, and the various

fitting procedures. The other significant component of the frequency uncertainties arises from the drift in the balance of the photodetectors and the offset voltages of the methane stabilization feedback electronics. We estimate that the zero crossing of the locking feature at 1314.588 nm was established and maintained to within an offset of 5-mV DC. Given the slopes of the derivative spectroscopy signals at the high and low pressures, the estimated offset corresponds to frequency uncertainties of 0.5 and 1.5 MHz, respectively. The low-pressure measurement has a greater uncertainty because of the weaker absorption. Instruments for measuring frequency were referenced to the microwave transition in cesium that forms the basis for the NIST atomic clock and contribute a negligible uncertainty. The change in the frequency shift caused by neighboring spectral features, a second-order effect, is negligible at the relatively low pressures involved. The two primary components of frequency uncertainty were combined in a root-sum-of-squares fashion and also converted to vacuum wavelength uncertainties.

The pressure uncertainties for the high- and low-pressure cells are estimated to be 0.38 kPa (2.9 torr) and 0.06 kPa (0.5 torr), respectively. The uncertainty values derive from the specified accuracy of the pressure gauge, and from the procedures for filling and sealing the cells. After filling, the mechanical o-ring valves of each cell were closed. In addition, the stem of the high-pressure cell was tipped off with a torch while the majority volume was immersed in liquid nitrogen to condense the gas. The final pressure and uncertainty were calculated based on the measured vapor pressure of methane and the change in cell volume.

Uncertainties for the extrapolated values at zero pressure were obtained with a Monte Carlo simulation using the data from the high- and low-pressure measurements. They depend on both the measured pressures and center frequencies (or wavelengths) as well as their respective uncertainties. By using the Monte Carlo technique, we were able to account for the correlations between the different quantities. The same technique was used to estimate the expanded ( $2\sigma$ ) uncertainty in the pressure shift value of 1.1 MHz/kPa (0.14 MHz/torr) that has already been mentioned.

#### IV. CONCLUSION

We have conducted a study of potential wavelength calibration references for use as moderate-accuracy transfer standards and high-accuracy NIST internal references in the 1280–1320-nm WDM region. Among the primary considerations were the availability of absorption lines, their strengths, the ease at which they could be probed, and the material handling issues. For our development of a NIST internal

high-accuracy reference, we avoided a number of candidates because they required an additional excitation step to probe upper-level transitions. Optical, electrical, or thermal excitation would have increased the experimental complexity and may shift the line centers. Materials that would have been difficult to obtain commercially or handle in the laboratory were also avoided. Another important consideration in selecting a material, particularly for a high-accuracy reference, was the uncertainty to which the position of the absorption lines had been previously measured. In the case of methane, we felt that the strength of the spectral features and the ease of handling justified the effort of additional measurements. Of course, the availability of the calcium-based optical frequency standard used in the measurements was also an important consideration. This resource provides an in-house calibration standard at 1314 nm with an uncertainty of 13 Hz, or fractionally  $6 \times 10^{-14}$ .

We developed a high-accuracy wavelength reference at 1314 nm by actively stabilizing a laser to a methane line and measuring the laser's frequency. This methane wavelength reference has been used in our laboratory to calibrate a wavelength meter having an uncertainty of  $1 \times 10^{-7}$ . However, the 30-MHz optical width of the wavelength reference, as shown in the mixed-down beat note of Fig. 4, can cause the last digit of the wavelength meter readings to fluctuate. We were able to overcome this noise, caused primarily by the dither of the laser's center wavelength, by averaging a sequence of readings. A more elegant solution to this problem would be to develop a dither-free wavelength reference using external frequency modulation [26]. Instead of applying the dither directly to the wavelength control of the laser, a small portion of the laser output is passed through an external frequency modulator driven by the dither signal. As before, the modulated light traverses the gas cell of the reference material and produces an error signal, which is conditioned and applied to the wavelength control of the laser. Once stabilized, the portion of the output that is not modulated is available for calibration purposes. We are investigating this technique and may implement it in the future.

## REFERENCES

- [1] S. L. Gilbert, W. C. Swann, and C. M. Wang, "Hydrogen cyanide  $H^{13}C^{14}N$  absorption reference for 1530–1560 nm wavelength calibration—SRM 2519," NIST Publication 260-137, 1998.
- [2] W. C. Swann and S. L. Gilbert, "Pressure-induced shift and broadening of 1510–1540-nm acetylene wavelength calibration lines," *J. Opt. Soc. Amer. B*, vol. 17, pp. 1263–1270, July 2000.
- [3] S. L. Gilbert and W. C. Swann, "Acetylene  $^{12}C_2H_2$  absorption reference for 1510 nm to 1540 nm wavelength calibration—SRM 2517a," NIST Publication 260-133, 2001.
- [4] T. Dennis, W. C. Swann, and S. L. Gilbert, "Wavelength references for 1300 nm and L-band WDM," in *OSA Trends in Optics and Photonics (TOPS) Vol. 54, Optical Fiber Communications Conference*, Tech. Dig., Postconference ed. Washington, DC, 2001, pp. WDD83-1–WDD83-3.
- [5] A. Bruner, V. Mahal, I. Kiryushev, A. Arie, M. A. Arbore, and M. M. Fejer, "Frequency stability at the kilohertz level of a rubidium-locked diode laser at 192.114 THz," *Appl. Opt.*, vol. 37, pp. 6410–6414, Sept. 1998.
- [6] H. Sasada, "Wavenumber measurements of sub-Doppler spectral lines of Rb at 1.3  $\mu$ m and 1.5  $\mu$ m," *IEEE Photon. Technol. Lett.*, vol. 4, pp. 1307–1309, Nov. 1992.
- [7] M. Breton, N. Cyr, P. Tremblay, M. Têtu, and R. Boucher, "Frequency locking of a 1324 nm DFB laser to an optically pumped rubidium vapor," *IEEE Trans. Instrum. Meas.*, vol. 42, pp. 162–166, Apr. 1993.

- [8] A. J. Lucero, Y. C. Chung, and R. W. Tkach, "Survey of atomic transitions for absolute frequency locking of lasers for lightwave systems," *IEEE Photon. Technol. Lett.*, vol. 3, pp. 484–486, May 1991.
- [9] V. Kaufman and B. Edlén, "Reference wavelengths from atomic spectra in the range 15 Å to 25 000 Å," *J. Phys. Chem. Ref. Data*, vol. 3, pp. 825–895, 1974.
- [10] Y. C. Chung, "Frequency locking of a 1.3  $\mu$ m DFB laser using a miniature argon glow lamp," *IEEE Photon. Technol. Lett.*, vol. 1, pp. 135–136, June 1989.
- [11] C. J. Sansonetti, "Precise measurements of hyperfine components in the spectrum of molecular iodine," *J. Opt. Soc. Amer. B*, vol. 14, pp. 1913–1920, Aug. 1997.
- [12] A. Arie, M. L. Bortz, M. M. Fejer, and R. L. Byer, "Iodine spectroscopy and absolute frequency stabilization with the second harmonic of the 1319-nm Nd:YAG laser," *Opt. Lett.*, vol. 18, pp. 1757–1759, Oct. 1993.
- [13] L. S. Rothman, R. L. Hawkins, R. B. Wattson, and R. R. Gamache, "Energy levels, intensities, and linewidths of atmospheric carbon dioxide bands," *J. Quant. Spectrosc. Radiat. Transf.*, vol. 48, pp. 537–566, 1992.
- [14] R. A. Toth, "Extensive measurements of  $H_2^{16}O$  line frequencies and strengths: 5750 to 7965  $cm^{-1}$ ," *Appl. Opt.*, vol. 33, pp. 4851–4867, July 1994.
- [15] K. Chan, H. Ito, and H. Inaba, "Absorption measurement of  $\nu_2 + 2\nu_3$  band of  $CH_4$  at 1.33  $\mu$ m using an InGaAsP light emitting diode," *Appl. Opt.*, vol. 22, pp. 3802–3804, Dec. 1983.
- [16] H. Kanamori, S. Takashima, and K. Sakurai, "Near-infrared diode laser spectrometer with frequency calibration using internal second harmonics," *Appl. Opt.*, vol. 30, pp. 3795–3798, Sept. 1991.
- [17] N. Moriwaki, T. Tsuchida, Y. Takehisa, and N. Ohashi, "1.3- $\mu$ m DFB diode laser spectroscopy of  $^{12}C_2H_2$ ," *J. Mol. Spectrosc.*, vol. 137, pp. 230–234, Sept. 1989.
- [18] M. de Labachellerie, K. Nakagawa, Y. Awaji, and M. Ohtsu, "High-frequency-stability laser at 1.5  $\mu$ m using Doppler-free molecular lines," *Opt. Lett.*, vol. 20, pp. 572–574, Mar. 1995.
- [19] E. Hirota, T. Ishiwata, K. Kawaguchi, M. Fujitake, N. Ohashi, and I. Tanaka, "Near-infrared band of the nitrate radical  $NO_3$  observed by diode laser spectroscopy," *J. Chem. Phys.*, vol. 107, pp. 2829–2838, Aug. 1997.
- [20] G. Guelachvili, "Absolute wavenumber measurements of 1-0, 2-0, HF and 2-0,  $H^{35}Cl$ ,  $H^{37}Cl$  absorption bands," *Opt. Commun.*, vol. 19, pp. 150–154, Oct. 1976.
- [21] S. Yamaguchi and M. Suzuki, "Frequency locking of an InGaAsP semiconductor laser to the first overtone vibration-rotation lines of hydrogen fluoride," *Appl. Phys. Lett.*, vol. 41, pp. 1034–1036, Dec. 1982.
- [22] A. D. Bykov, O. V. Naumenko, M. A. Smirnov, L. N. Sinita, L. R. Brown, J. Crisp, and D. Crisp, "The infrared spectrum of  $H_2S$  from 1 to 5  $\mu$ m," *Can. J. Phys.*, vol. 72, pp. 989–1000, Nov.–Dec. 1994.
- [23] K. Suzumura, C. Ishibashi, and H. Sasada, "Precise frequency-difference measurement between the 1.66  $\mu$ m transitions of methane," *Opt. Lett.*, vol. 22, pp. 1356–1358, Sept. 1997.
- [24] C. W. Oates, F. Bondu, R. W. Fox, and L. Hollberg, "A diode-laser optical frequency standard based on laser-cooled Ca atoms: Sub-kilohertz spectroscopy by optical shelving detection," *Eur. Phys. J. D*, vol. 7, pp. 449–460, Jan. 1999.
- [25] Th. Udem, S. A. Diddams, K. R. Vogel, C. W. Oates, E. A. Curtis, W. D. Lee, W. M. Itano, R. E. Drullinger, J. C. Bergquist, and L. Hollberg, "Absolute frequency measurements of the  $Hg^+$  and Ca optical clock transitions with a femtosecond laser," *Phys. Rev. Lett.*, vol. 86, pp. 4996–4999, May 2001.
- [26] G. C. Bjorklund, "Frequency-modulation spectroscopy: A new method for measuring weak absorptions and dispersions," *Opt. Lett.*, vol. 5, pp. 15–17, Jan. 1980.

**T. Dennis**, photograph and biography not available at the time of publication.

**E. A. Curtis**, photograph and biography not available at the time of publication.

**C. W. Oates**, photograph and biography not available at the time of publication.

**L. Hollberg** (A'92), photograph and biography not available at the time of publication.

**S. L. Gilbert**, photograph and biography not available at the time of publication.